Biophysical Journal
Article

Biophysical Society

Polyunsaturated Lipids Regulate Membrane Domain Stability by Tuning Membrane Order

Kandice R. Levental,[1] Joseph H. Lorent,[1] Xubo Lin,[1] Allison D. Skinkle,[2] Michal A. Surma,[3] Emily A. Stockenbojer,[2] Alemayehu A. Gorfe,[1] and Ilya Levental[1,*]
[1]Department of Integrative Biology and Pharmacology, University of Texas Health Science Center at Houston, Houston, Texas; [2]Department of Biochemistry and Cell Biology, Rice University, Houston, Texas; and [3]Lipotype GmbH, Dresden, Germany

ABSTRACT The plasma membrane (PM) serves as the functional interface between a cell and its environment, hosting extracellular signal transduction and nutrient transport among a variety of other processes. To support this extensive functionality, PMs are organized into lateral domains, including ordered, lipid-driven assemblies termed lipid rafts. Although the general requirements for ordered domain formation are well established, how these domains are regulated by cell-endogenous mechanisms or exogenous perturbations has not been widely addressed. In this context, an intriguing possibility is that dietary fats can incorporate into membrane lipids to regulate the properties and physiology of raft domains. Here, we investigate the effects of polyunsaturated fats on the organization of membrane domains across a spectrum of membrane models, including computer simulations, synthetic lipid membranes, and intact PMs isolated from mammalian cells. We observe that the ω-3 polyunsaturated fatty acid docosahexaenoic acid is robustly incorporated into membrane lipids, and this incorporation leads to significant remodeling of the PM lipidome. Across model systems, docosahexaenoic acid-containing lipids enhance the stability of ordered raft domains by increasing the order difference between them and coexisting nonraft domains. The relationship between interdomain order disparity and the stability of phase separation holds for a spectrum of different perturbations, including manipulation of cholesterol levels and high concentrations of exogenous amphiphiles, suggesting it as a general feature of the organization of biological membranes. These results demonstrate that polyunsaturated fats affect the composition and organization of biological membranes, suggesting a potential mechanism for the extensive effects of dietary fat on health and disease.

INTRODUCTION

Membrane rafts are believed to be a central mechanism for functional partitioning of the plasma membrane (PM) (1). These domains are believed to comprise a major fraction (2), if not the majority (3,4), of the surface of the PM, and therefore it is unsurprising that they have been implicated in nearly all aspects of membrane physiology. The cellular processes most commonly associated with membrane domains involve extracellular signal transduction through surface-bound receptors. Lateral membrane domains have been proposed to serve as reaction vessels, selectively recruiting membrane components (e.g., membrane receptors and their second messengers) to facilitate their interactions and/or prevent interaction with negative regulators (5). However, it is important to emphasize that this cartoon model does not capture the inherently probabilistic nature of both protein-protein interactions and the recruitment of proteins by membrane domains, as both protein residence within a domain and the domain itself are expected to be transient, even on the timescale of molecular interactions.

Because of their inherent transience and relatively weak protein selectivity (1,6), raft domains likely serve as modulators rather than intrinsic components of signaling processes. The most commonly considered mode of such modulation is the regulated recruitment of specific proteins to raft domains, with the raft association (e.g., from nonraft to raft) of a given protein regulating its interaction with an effector (7,8). However, a less widely explored potential model of raft-mediated signaling holds that changes in the properties of the domains themselves, such as their size, lifetime, and/or order, occur during cellular processes. As these properties ultimately determine the timescales and length scales of raft-associated processes, their regulation may be a powerful mechanism to tune the output of a variety of signaling modules (9–11). Unfortunately, the properties of membrane domains in live cells remain generally inaccessible to modern methodologies, although recent

Submitted October 29, 2015, and accepted for publication March 9, 2016.
*Correspondence: ilya.levental@uth.tmc.edu
Editor: Scott Feller.
http://dx.doi.org/10.1016/j.bpj.2016.03.012

applications of superresolution correlation microscopy (12) and spectroscopy (13,14) hold great promise.

Because of the relative intractability of membrane domains in live cells, an important breakthrough has been the observation and characterization of coexisting raft and nonraft domains in intact PMs isolated as giant PM vesicles (GPMVs) (15–17). Conceptually, the formation of selective (6), ordered (18), lipid-driven domains in biologically derived membranes is a critical confirmation of the potential for such domain formation in live cells. It is important to note that there are several important differences between PMs in live cells and isolated GPMVs (16,17,19), including the loss of strict membrane asymmetry (15) and degradation of some lipids during GPMV formation (20). Although the potential effects of these differences on membrane physical properties have not been resolved, GPMVs provide a valuable experimental system for characterizing biophysical properties in membranes of biological complexity and composition. A number of recent reports have characterized regulators of phase behavior in GPMVs, including protein-lipid binding/oligomerization (21), expression of specific proteins (22), bile acid incorporation into the membranes (23), various general liquid anesthetics (24), and the specific protocols used to isolate the GPMVs (25). The stability of domain separation in GPMVs seems to be related to the relative composition and physical properties of the coexisting domains, as evidenced by changes in raft domain order associated with their overall protein content (25). Although this effect (i.e., broad depletion of raft proteins) is almost certainly unphysiological, it demonstrates that the raft domain order and the relative properties of coexisting domains are potential determinants of raft stability. This hypothesis recently received validation in synthetic membranes (26).

The relationships between domain properties and composition in biomimetic synthetic membranes have been extensively investigated (27–29). In contrast, the mechanisms by which domain properties are regulated in biological membranes remain almost wholly unknown. Although acute wholesale changes to membrane composition are likely rare, an intriguing possibility is that cell membrane composition in vivo is susceptible to long-term modulation by dietary fats, including both cholesterol (Chol) and fatty acids (FAs). Of specific interest is the ω-3 polyunsaturated FA (PUFA) docosahexaenoic acid (DHA), a fish oil component whose consumption is associated with a variety of health benefits, particularly antiinflammatory (30) and cardioprotective effects (31). Dietary DHA can incorporate into cellular PMs in vivo (32) and potentially affect the physical properties of membranes (33) and the organization of domains therein (28,29). Model membrane experiments and simulations suggest that these lipids have highly unfavorable interactions with Chol (34–37) and do not pack into ordered phases (35,38), instead forming PUFA-lipid-rich, highly disordered domains (35,39). A recent NMR study confirmed that DHA-containing lipids enhance phase separation in raft-mimetic model membranes (40). Another study proposed an alternative mechanism whereby PUFA-containing lipids infiltrate Chol-rich ordered domains (41) to potentially disrupt their packing. Such infiltration has been inferred by NMR and is consistent with the presence of PUFA-containing lipids in detergent-resistant membranes from cells (42).

Here, we investigate the effects of dietary fats and exogenous amphiphiles on the organization of membrane domains across a spectrum of membrane models, including coarse-grained (CG) molecular-dynamics (MD) simulations, synthetic pure-lipid membranes, and intact PMs isolated directly from mammalian cells. Our results show that supplementation with physiologically relevant concentrations of ω-3 DHA leads to its robust incorporation into specific PM lipid types and induces a profound remodeling of the PM lipidome. The biophysical consequence of lipidomic remodeling is stabilization of membrane domains via the disordering of nonraft domains by polyunsaturated lipids. We confirm these effects in both synthetic membranes and simulations. Finally, this correlation between the interdomain order differential and the stability of liquid-liquid phase separation persists across a variety of membrane perturbations, suggesting that this relationship is a general design feature of biological membranes.

MATERIALS AND METHODS

Materials

The following materials were purchased for this study: sodium deoxycholate (DCA; Sigma, St. Louis, MO), Triton X-100 (Thermo Fisher, Waltham, MA), *cis*-4,7,10,13,16,19-docosahexaenoic acid (DHA; Sigma), oleic acid (OA; Sigma), methyl-β-cyclodextrin (MBCD; Sigma), and Fast DiO (Life Technologies, Carlsbad, CA). The following antibodies were used: LAT (polyclonal; Cell Signaling, Danvers, MA), Na^+/K^+ ATPase (polyclonal; Cell Signaling), Sec61a (monoclonal; Abcam, Cambridge, MA), Calnexin (polyclonal; Abcam), Hexokinase (monoclonal; Cell Signaling), LAMP1 (polyclonal, Abcam), GOLGA7 (monoclonal, Abcam), Rab5 (polyclonal; Cell Signaling), Alexa Fluor 488 goat anti-rabbit (Life Technologies), and Alexa Fluor 633 goat anti-rabbit (Life Technologies). The following lipids were purchased from Avanti Polar Lipids, Alabaster, AL: chicken egg sphingomyelin (SM), 1-palmitoyl-2-oleoylphosphatidylcholine (POPC), 1,2-dioleoyl PC (DOPC), 1-stearoyl-2-docosahexaenoyl PC (SDPC), Chol, and fluorescent rhodamine-DPPE.

Cell culture and treatment

Rat basophilic leukemia (RBL) cells were maintained in medium containing 60% modified Eagle's medium (MEM), 30% RPMI, 10% fetal calf serum, 2 mM glutamine, 100 units/mL penicillin, and 100 μg/mL streptomycin at 37°C in humidified 5% CO_2.

For all experiments with FA (DHA, OA, or arachidonic acid) supplementation, cells were incubated with 20 μM FA for 4 days (supplemented every 2 days). This concentration was chosen to approximate conditions observed in vivo under DHA-enriched diets: plasma free FA concentrations range from 300 to 750 μM (43,44) and up to 10 mol % of plasma fatty acids

are ω-3 DHA in rats fed a high-fish-oil diet (43). Further, diets rich in ω-3 PUFAs led to significant incorporation of these fats into cell membrane lipids (32,43,45), similar to the levels we observed under our culture feeding conditions (Fig. 1). For these reasons, we believe our culture conditions reasonably approximate physiological DHA supplementation.

FA stock solutions were received as air-purged ampules and loaded into bovine serum albumin (BSA) immediately upon opening. BSA loading was accompanied by stirring the FA with BSA dissolved in water (2:1 mol/mol FA/BSA), sterile filtering, purging with nitrogen before aliquoting, and storage at −80°C. BSA loading, purging, and cold storage were all done to minimize FA oxidation. Lipid peroxidation was measured by the ferrous oxidation in a xylenol orange (FOX) assay as previously described (46), and no lipid peroxide signal was detectable in any of the FA stocks. Chol depletion was accomplished by incubating the cells with MBCD for 30 min in Dulbecco's MEM before GPMV isolation.

GPMV isolation

GPMVs were isolated and imaged as previously described (15,16,19). Briefly, cells were washed in GPMV buffer (10 mM HEPES, 150 mM NaCl, 2 mM $CaCl_2$, pH 7.4) and then incubated with GPMV buffer supplemented with 25 mM paraformaldehyde and 2 mM dithiothreitol (or 2 mM N-ethylmaleimide for lipidomic experiments) for 1 h at 37°C. Before isolation, cell membranes were labeled with 5 μg/mL of the fluorescent disordered/nonraft phase marker FAST DiO for 10 min on ice. Triton X-100 or DCA treatment was accomplished by treating the GPMV solution with the indicated concentration of Triton X-100 or DCA, respectively, for 30 min before imaging. Vesicles were imaged at 40× on an inverted epifluorescence microscope (Nikon, Melville, NY) under temperature-controlled conditions using a microscope stage equipped with a Peltier element (Warner Instruments, Hamden, CT).

Quantification of miscibility transition temperatures

Miscibility transition temperatures (T_{misc}) were quantified as previously described (2,16,19). Briefly, phase separation was microscopically assessed for >50 vesicles/temperature and the fraction of phase-separated vesicles plotted against temperature was fit with a sigmoidal curve (see Fig. 2 *B*). The point of the curve representing 50% phase-separated vesicles was defined as T_{misc}.

Lipidomics

Membrane isolation

For lipidomic analysis of isolated PMs, GPMVs were prepared after 4 days of treatment with DHA or OA. Cells were washed with GPMV buffer and incubated with 2 mM N-ethylmaleimide in GPMV buffer for 1 h at 37°C. Whole-cell contamination was removed by a short, low-speed centrifugation (3 min at 300 *g*) and the GPMVs remaining in the supernatant were pelleted by centrifugation (20,000 *g* for 1 h at 4°C), washed, and resuspended in 150 mM ammonium bicarbonate.

To prepare crude cell membranes, cells were washed with phosphate-buffered saline (PBS), scraped in 10 mM Tris pH 7.4, and then homogenized with a 27-gauge needle. Nuclei were then pelleted by centrifugation at 300 *g* for 5 min. The supernatant was pelleted by centrifugation at 100,000 *g* for 1 h at 4°C. The membrane pellet was then washed and resuspended in 150 mM ammonium bicarbonate.

Lipids

The following lipids were used: ceramide (Cer), Chol, SM, diacylglycerol (DAG), lactosyl ceramide (DiHexCer), glucosyl/galactosyl ceramide (HexCer), sterol ester (SE), and triacylglycerol (TAG), as well as phosphatidic acid (PA), phosphatidylcholine (PC), phosphatidylethanolamine (PE), phosphatidylglycerol (PG), and phosphatidylinositol (PI), phosphatidylserine (PS), and their respective lysospecies (lysoPA, lysoPC, lysoPE, lysoPI, and lysoPS) and ether derivatives (PC O-, PE O-, LPC O-, and LPE O-).

Lipid species were annotated according to their molecular composition as follows: [lipid class]-[sum of carbon atoms in the FAs]:[sum of double bonds in the FAs];[sum of hydroxyl groups in the long chain base and the FA moiety] (e.g., SM-32:2;1). When available, the individual FA composition according to the same rule is given in brackets (e.g., 18:1; 0-24:2;0).

Lipid extraction

Samples were extracted and analyzed as previously described (39,47), which is a modification of a previously published method for shotgun

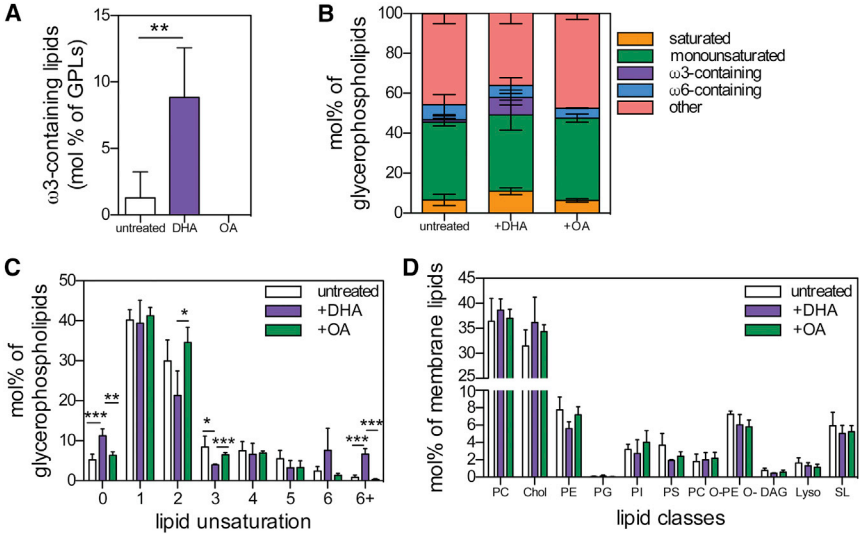

FIGURE 1 Lipidomic remodeling of PMs by DHA supplementation. PMs were isolated from cultured RBLs as GPMVs and analyzed by mass spectrometric lipidomics. (*A*) Supplementation with 20 μM DHA led to robust incorporation of this ω-3 PUFA into membrane lipids: although DHA-containing lipids were nearly undetectable in control or OA-fed cells, they comprised ~8 mol % of all glycerophospholipids after DHA supplementation. (*B*) Stacked bar chart illustrating the distribution of various glycerophospholipid classes as a function of FA supplementation and the increase in ω-3 PUFA-containing lipids by DHA supplementation. (*C*) Levels of fully saturated lipids were significantly increased in DHA-treated PMs, whereas lipids containing two or three unsaturations were significantly reduced. As expected, lipids containing six or more unsaturations were also increased by DHA supplementation. OA supplementation had little notable effect on PM lipidomes. (*D*) FA supplementation had little notable effect on the headgroup distribution of the lipidome. All data are mean ± SD from at least three independent experiments and were analyzed by Student's *t*-test. $*p < 0.05$, $**p < 0.01$, $***p < 0.001$. To see this figure in color, go online.

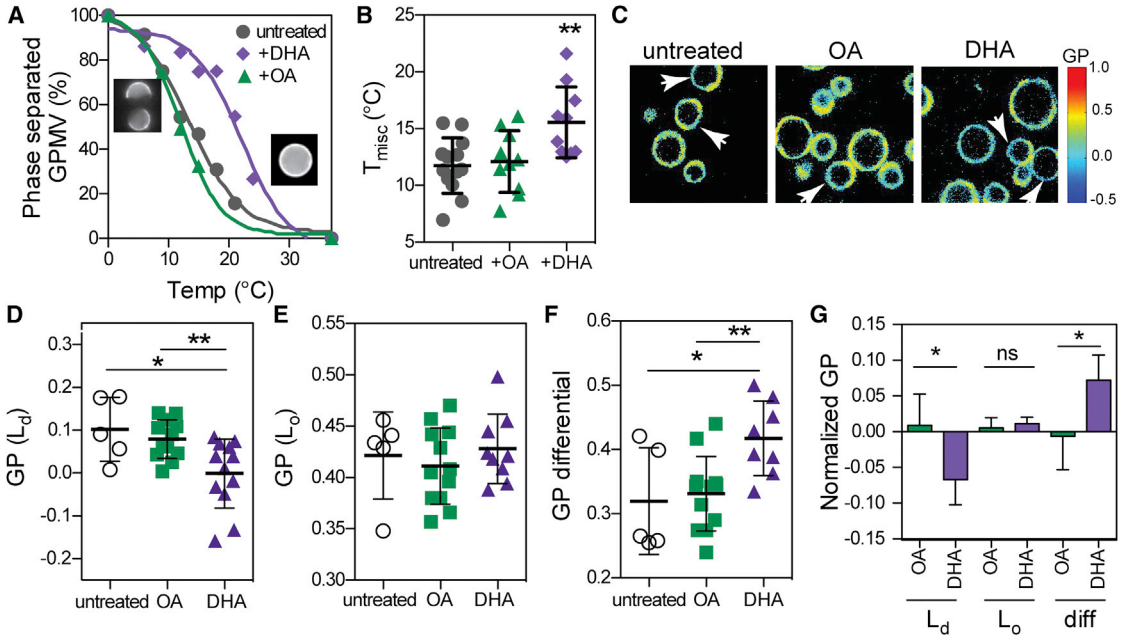

FIGURE 2 Effect of DHA-induced lipidomic remodeling on phase behavior in isolated PMs. (*A*) Representative curves show that DHA supplementation produces a rightward shift of the phase separation curve in GPMVs, indicative of more stable phase separation. Curves were generated by counting >50 vesicles/temperature/condition. (*B*) DHA supplementation significantly increases T_{misc}, whereas OA has no effect. Mean ± SD of ≥10 experiments; $^{**}p < 0.01$. (*C*) Exemplary GP maps of C-laurdan used to visualize the order of coexisting domains in phase-separated GPMVs. Arrowheads identify the relatively disordered (L_d) domains, and cooler colors in DHA supplementation are indicative of increased disorder. Scale bar, 5 μm. (*D* and *E*) L_d domains in GPMVs are significantly disordered by DHA supplementation (*D*), whereas the ordered (L_o) domains are unaffected (*E*). (*F*) The GP differential between phases is significantly increased by DHA supplementation. Data in (*D–F*) are mean ± SD from one experiment of 10–15 vesicles/condition, representative of four independent repeats. (*G*) Normalized means ± SD from all four independent experiments. The GP values were normalized to the untreated values in each individual experiment. This was done to account for nonnegligible differences in absolute GP values between experiments, which we attributed to variations in detector efficiencies between the two channels in the GP imaging experiments. $^{*}p < 0.05$, $^{**}p < 0.01$. To see this figure in color, go online.

lipidomics (48). Briefly, membrane samples were suspended in 150 μL of 150 mM ammonium bicarbonate in water, spiked with 20 μL of internal standard lipid mixture, and then extracted with 750 μL of a chloroform/methanol 10:1 (v/v) mixture for 2 h at 4°C with 1400 rpm shaking. After centrifugation (3 min, 3000 *g*) to facilitate phase partitioning, the lower, lipid-containing, organic phase was collected (first-step extract), and the remaining water phase was further extracted with 750 μL of a chloroform/methanol 2:1 (v/v) mixture under the same conditions. Again the lower, organic phase was collected (second-step extract). Extracts were dried in a speed vacuum concentrator, and 120 μL of a dried first-step extract underwent acetylation with 75 μL of an acetyl chloride/chloroform 1:2 (v/v) mixture for 1 h to derivatize Chol. After the reaction was completed, the mixture was dried. Then, 120 μL of a dried first-step extract and a derivatized extract were resuspended in an acquisition mixture with 8 mM ammonium acetate (400 mM ammonium acetate in methanol/chloroform/methanol/propan-2-ol, 1:7:14:28, v/v/v/v). Next, 120 μL of the second-step extract was resuspended in an acquisition mixture with 30 μL 33% methylamine in methanol, in 60 mL methanol/chloroform 1:5 (v/v). All liquid-handling steps were performed using a Hamilton (Reno, NV) STARlet robotic platform with the Anti Droplet Control feature, ensuring the accuracy and reproducibility of organic solvent pipetting.

Lipid standards

Synthetic lipid standards were purchased from Sigma-Aldrich (Chol D6), Larodan (Solna, Sweden) Fine Chemicals (DAG and TAG), and Avanti Polar Lipids (all others). The standard lipid mixtures were chloroform/methanol 1:1 (v/v) solutions containing Cer 35:1;2, (D18:1;2, 17:0;0); Chol D6; DAG 34:0;0 (17:0;0, 17:0;0); DiHexCer 30:1;2 (D18:1;2.12:0;0); HexCer 30:1;2 (D18:1;2.12:0;0); LPA 17:0;0 (17:0;0); LPC 12:0;0 (12:0;0); LPE 17:1;0 (17:1;0); LPI 17:1;0 (17:1;0); LPS 17:1;0 (17:1;0); PA 34:0;0 (17:0;0, 17:0;0); PC 34:0;0 (17:0;0, 17:0;0); PE 34:0;0 (17:0;0, 17:0;0); PG 34:0;0 (17:0;0, 17:0;0); PI 32:0;0 (16:0;0, 16:0;0); PS 34:0;0 (17:0;0, 17:0;0); SE 20:0;0 (20:0;0); SM 30:1;2 (18:1;2, 12:0;0); and TAG 51:0;0 (17:0;0, 17:0;0, 17:0;0).

Lipid spectrum acquisition

Extracts in the acquisition mixtures were infused with a robotic nanoflow ion source (TriVersa NanoMate; Advion Biosciences, Ithaca, NY) into a mass spectrometer instrument (Q Exactive, Thermo Scientific). Cer, DiHexCer, HexCer, lysolipids, and SM were monitored by negative ion mode Fourier transform mass spectrometry (FT-MS). PA, PC, PE, PI, PS, and ether species were monitored by negative ion mode FT tandem MS (FT-MS/MS). Acetylated Chol was monitored by positive ion mode FT-MS. SE, DAG, TAG, and species were monitored by positive ion mode FT-MS/MS.

Lipid identification and quantification

Automated processing of acquired mass spectra, and identification and quantification of detected molecular lipid species were performed with the use of LipidXplorer software (17). Only lipid identifications with a signal/noise ratio of >5, an absolute abundance of at least 1 pmol, and a signal intensity fivefold higher than in the corresponding blank samples were considered for further data analysis.

Western blotting for organelle contamination in GPMV preparations

GPMVs or crude membrane preparations were lysed in Laemmli lysis buffer (50 mM Tris-HCl, pH 8.0; 2% SDS; 5 mM EDTA, pH 7.4) supplemented with a protease inhibitor cocktail. The protein concentration was determined using a bicinchoninic acid assay (Pierce), and equal volumes were mixed with reducing Laemmli sample buffer and loaded onto SDS-PAGE gels. Gels were transferred to PVDF membranes that were blocked in 5% milk-TBST. Membranes were incubated with primary antibodies either overnight at 4°C or for 2 h at room temperature on a rocker, washed with TBST, and incubated with either Alexa Fluor or horseradish peroxidase-tagged secondary antibodies for 1 h before visualization.

Preparation of giant unilamellar vesicles

Giant unilamellar vesicles (GUVs) were prepared using the electroformation method as previously described (49). Briefly, 1 μL of a chloroform/methanol (2:1 v/v) solution containing 5 mg/mL of lipids was spread on both platinum electrodes of a Teflon-electroformation chamber. The solvent was dried to form a lipid film on the platinum electrodes by evaporating the solution in a vacuum chamber for 1 h. The electroformation solution was 350 μL of a 0.1 M sucrose solution. The GUVs were grown by applying a sinusoidal alternating current of 10 Hz and 2.5 V for 2 h at 52°C. Rhodamine-DPPE (Avanti) was added to the lipid mix at 0.1 mol % to visualize phase separation, due to its preference for the disordered phase. When necessary, C-laurdan (a kind gift from Dr. Bong Rae Cho) was included at 0.5 mol % for GP imaging.

Preventing and measuring lipid oxidation during GUV preparation and visualization

For GUV preparation, metal electrodes were used rather than indium-tin-oxide coverslips because this method has been shown to minimize lipid oxidation during GUV formation (46). Further, the antioxidant N-propyl gallate (NPG) was included in the electroformation solution (0.2 mM NPG). We used the FOX assay to quantify the effectiveness of these steps for preventing lipid oxidation, and observed no detectable lipid peroxide signal in any of our GUV preparations (Fig. S4 in the Supporting Material). Control experiments confirmed that NPG at this concentration had no effect on ΔT_{misc}. During imaging, we were careful to minimize exposure to intense excitation light and ensure that none of the observed effects were associated with illumination, for example, by measuring whether T_{misc} values remained stable after illumination and whether domains appeared/disappeared during isothermal illumination.

C-laurdan spectroscopy

Membrane order was determined via C-laurdan spectroscopy as previously described (16,19). Briefly, cells were washed with PBS and stained with 20 μg/mL C-laurdan for 10 min on ice. The emission spectrum from isolated GPMVs was gathered from 400 to 550 nm with excitation at 385 nm at 23°C. The GP was calculated according to the following equation:

$$GP = \frac{\sum_{420}^{460} I_x - \sum_{470}^{510} I_x}{\sum_{420}^{460} I_x + \sum_{470}^{510} I_x}.$$

C-laurdan microscopy

Cells were washed with PBS and stained with 10 μg/mL C-laurdan for 10 min on ice. GPMVs were collected and imaged via confocal microscopy on a Nikon A1R with spectral imaging at 60× and an excitation of 405 nm at 10°C. The emission was collected in two bands: 433–463 nm and 473–503 nm. MATLAB (The MathWorks, Natick, MA) was used to calculate the two-dimensional (2D) GP map, where GP for each pixel was calculated from a ratio of the two fluorescence channels as previously described (50). Briefly, each image was binned (2 × 2), background subtracted, and thresholded to keep only pixels with intensities greater than 3 standard deviations of the background value in both channels. The GP image was calculated for each pixel using the equation above. The GP of each phase (disordered and ordered) was calculated by averaging pixels from a large representative area of both phases. The ΔGP was determined for each vesicle rather than for populations.

MD simulations

Model membranes were simulated using the MARTINI CG force field (v.2.1) (51,52). Initially, randomly distributed membrane systems were built by randomly placing all lipids and equilibrating the system at $T = 400$ K for 100 ns. The two systems consisted of 368 DPPC, 368 POPC/1-palmitoyl-2-docosahexaenoyl PC (POPC/PDPC), 368 Chol, 23,674 CG water, and 0.15 mM Na^+/Cl^-.

For all simulations, a cutoff of 1.2 nm was used for van der Waals interactions, and the Lennard-Jones potential was smoothly shifted to zero between 0.9 nm and 1.2 nm to reduce cutoff noise. For electrostatic interactions, the Coulomb potential, with a cutoff of 1.2 nm, was smoothly shifted to zero from 0 to 1.2 nm. The relative dielectric constant was 15, the default value of the force field (51). Lipids and water ions were coupled separately to V-rescale heat baths (53) at $T = 298$ K, with a coupling constant $\tau = 1$ ps. The systems were simulated at 1 bar pressure using a semi-isotropic Parrinello-Rahman pressure-coupling scheme (54) with a coupling constant $\tau = 1$ ps and compressibility of $3e^{-4}$ bar^{-1}. The neighbor list for nonbonded interactions was updated every 10 steps with a 1.4 nm cutoff. All of the simulations were performed for 32 μs (4 × 8 μs effective time) with a time step of 20 fs and periodic boundary conditions using GROMACS 4.5.4 (55). Snapshots of the simulation system used in this work were all rendered by VMD (56).

RESULTS AND DISCUSSION

Dietary fats are widely implicated in human health and disease, and in particular numerous beneficial effects have been ascribed to ω-3 PUFAs such as DHA (30,57). Remarkably, there remains no consensus regarding the mechanism(s) of action for the many physiological and cellular effects of ω-3 PUFAs (38,39). Here, we show that DHA is incorporated into membrane lipids, leading to compositional and biophysical remodeling of PMs.

FA supplementation leads to incorporation of ω-3 PUFAs into membrane lipids and remodeling of membrane lipidomes

To test the incorporation of exogenous DHA into membrane lipids, we supplemented the culture media of a model mammalian cell line (RBL) with either DHA or monounsaturated OA (18:1 ω-9) as 20 μM complexes with BSA and used shotgun lipidomics to measure the resulting effects on PM lipidomes (see Materials and Methods for details). PMs were isolated using the GPMV procedure, which was validated as being a highly PM-enriched preparation

(Fig. S1). We observed a remarkable incorporation of supplemented DHA into PM lipids. Although only a minimal amount of DHA-containing lipids was detected in control or OA-supplemented PMs, in DHA-supplemented cells, DHA was incorporated into 8.8 mol % of all PM phospholipids (Fig. 1 *A*; detailed lipid analysis shown in Fig. S3). DHA incorporation was highly headgroup specific: 62% of all DHA-containing lipids bore an ethanolamine headgroup and the majority of these (83%) contained the other FA linked via an ether bond, likely PE plasmalogens (Fig. S2). In addition to DHA incorporation, there was a notable remodeling of the membrane lipidomes in response to DHA supplementation, as evidenced by 1) increased saturated phospholipids (Fig. 1, *B* and *C*), 2) decreased di- and triunsaturated lipids (Fig. 1 *C*), and 3) increased ω-3 PUFA-containing lipids (Fig. 1 *B*).

Remarkably, control experiments with OA showed that monounsaturated FA supplementation had little effect on PM lipidomes (Fig. 1). We speculate that the divergent effects of DHA versus OA reflect the fact that ω-3 PUFAs are a limiting component in serum-containing cell culture media, whereas the abundance of OA is sufficient to meet normal demands, i.e., that cultured cells are effectively starved of PUFAs under standard culture conditions. This hypothesis remains to be explored.

DHA supplementation stabilizes membrane domains in GPMVs by increasing interdomain order disparity

The marked effects of DHA supplementation on PM lipid composition prompted us to investigate the biophysical consequences of these perturbations. Specifically, we focused on the stability of observable raft domains in isolated PMs, quantified as the temperature at which microscopic domains were observed in 50% of GPMVs, i.e., the T_{misc} (Fig. 2, *A* and *B*) (16,19). Supplementation with DHA significantly increased T_{misc}, whereas addition of monounsaturated OA had no significant effect. The enhancement of phase separation by DHA lipids is broadly consistent with previous reports on the stabilization of raft phases in vivo by diets rich in fish oil (42,58) or by genetic alterations designed to increase PUFA levels (59). The magnitude of the DHA effect (~6°C) was surprising in light of previous observations of more subtle effects on protein-mediated lipid clustering on phase separation in GPMVs (21). Indeed, the PUFA effects are more in line with major membrane perturbations induced by bile acids and liquid anesthetics (23,24).

Phase separation in model membranes has previously been related to the magnitude of the difference in physical properties between coexisting domains (23,25,26). To investigate whether such an effect was responsible for the stabilization of PM domains by PUFA supplementation, we imaged the order of coexisting domains in GPMVs by C-laurdan spectral microscopy (60). The fluorescence emission spectrum of laurdan (and its more hydrophilic analog C-laurdan (61)) is dependent on lipid packing and produces a progressively red-shifted emission with increasing membrane disorder (62), a property that is quantified by the dimensionless ratio generalized polarization (GP). Spectral imaging microscopy allows pixel-by-pixel resolution of these spectra and the generation of 2D GP maps that are reflective of relative membrane order/packing (63). We observed well-separated membrane domains of two different order values, confirming ordered/disordered phase separation in GPMVs (Fig. 2 *C*). The order of the relatively disordered domains was reduced in GPMVs isolated from DHA-supplemented cells, whereas OA supplementation had no effect (Fig. 2 *D*). The ordered domains were not affected by any of the treatments (Fig. 2 *E*). Together, these effects yielded a significantly enhanced order disparity between coexisting domains in DHA-treated GPMVs compared with untreated or OA-supplemented GPMVs (Fig. 2 *F*), which is fully consistent with previous NMR measurements in synthetic membranes (35). The robust disordering effect of PUFA-containing lipids on the liquid-disordered (L_d) phase and the lack of effect on the liquid-ordered (L_o) phase favor a model wherein the polyunsaturated lipids enrich in and affect the properties of nonraft domains (35,39), as opposed to the alternative possibility that PUFA lipids infiltrate and disrupt ordered domains (41). Our interpretation is similar to the "push-pull" mechanism for ordered domain formation that was proposed based on experimental observations of pairwise interaction parameters between lipids (64,65). However, we emphasize that we made no direct measurements of membrane domain composition, and thus our experiments could not directly distinguish the specific mechanisms of enhanced phase separation.

Surprisingly, we observed no significant effects on overall PM lipid packing (Fig. S7). We speculate that the above-described changes to the overall lipidome aside from PUFA incorporation (Fig. 1, *B* and *C*) compensate for the disordering effect of PUFA-containing lipids to maintain constant overall lipid packing.

DHA-containing lipids stabilize phase separation in GUVs by disordering the L_d phase

GPMVs are an ideal model system for investigating biophysical parameters in biological membranes. However, the lipid and protein complexity of these vesicles and the many possible cellular effects associated with DHA feeding prohibit a definitive assignment of our observations to the effect of DHA incorporation into lipids. To directly test the relationship between ω-3 PUFA-containing lipids and L_o/L_d phase separation, we investigated phase separation and membrane order in well-defined synthetic model membranes. GUVs were prepared from a mixture of saturated

sphingomyelin (SM, 33 mol %), mono- and diunsaturated phosphatidylcholine (POPC 16 mol % and DOPC 16 mol %, respectively), and 33 mol % Chol. Multiple steps were taken to avoid lipid oxidation during storage and GUV production, and these were effective in preventing oxidation (see Materials and Methods; Fig. S4). The particular lipid mixture was chosen to approximately mimic the acyl chain distribution in the PM lipidomes while eliminating any complications from charged headgroups. As expected (66), this mixture showed macroscopic separation into large liquid domains with a T_{misc} of ~30°C (Fig. 3 *A*). To assess the effect of DHA-containing lipids, 3 or 5 mol % of the POPC was replaced by 1-stearoyl-2-docosahexaenoyl PC (SDPC), i.e., switching the unsaturated chain from OA to DHA. The effect of this relatively minor change was a significant stabilization of phase separation in GUVs, with as little as 3 mol % SDPC increasing the T_{misc} by ~8°C (Fig. 3 *B*).

As in the GPMVs (Fig. 2, *D–F*), the root of this stabilization of phase separation appears to be disordering of the L_d phase by DHA-containing lipids, as evidenced by spectral microscopy of GUVs. The GP of the disordered phase was reduced in both DHA-containing mixtures by ~0.05 (Fig. 3 *C*), whereas there was little difference in the L_o phases of the 5% DHA mixture (Fig. 3 *D*), which increased the GP difference between the phases (Fig. 3 *E*). An interesting observation was the pronounced reduction in L_o phase order in GUVs containing 3% SDPC. This observation is in agreement with the above-referenced notion that PUFA lipids may partition into and disrupt ordered domains (41). However, the effect seems to be extremely context dependent, as it was not observed in GPMVs or in GUVs with 5% SDPC. Surprisingly, although these results from synthetic membranes qualitatively confirmed those obtained in the natural GPMVs, the effects of DHA in GUVs were less pronounced. We speculate that the more robust effects in GPMVs were due to the DHA-associated lipidomic remodeling, which was not recapitulated in the GUVs.

Dynamic molecular modeling confirms DHA-mediated disordering and enhanced domain separation

To validate the conclusions we drew from experiments in synthetic and natural model membranes, we performed CG MD simulations of mixed model membranes using the MARTINI force field, which has been widely used for simulations of phase separation in biomimetic membranes (67–69). As in the GUV experiments, we compared a standard "raft" mixture (equimolar DPPC/POPC/Chol) with a similar mixture wherein the monounsaturated POPC was replaced by PDPC (simulation details in Materials and Methods).

The snapshots in Fig. 4 *A* have been color-coded to show ordered lipids (DPPC/Chol) in black and disordered (POPC/PDPC) in white to highlight the ordered and disordered domains, respectively (full color image in Fig. S5). Whereas the DPPC/POPC/Chol system failed to evolve large domains during the simulation period, replacement of POPC by PDPC yielded a clear coarsening and separation of ordered and disordered domains. This was further evidenced by the increased likelihood of DPPC-DPPC

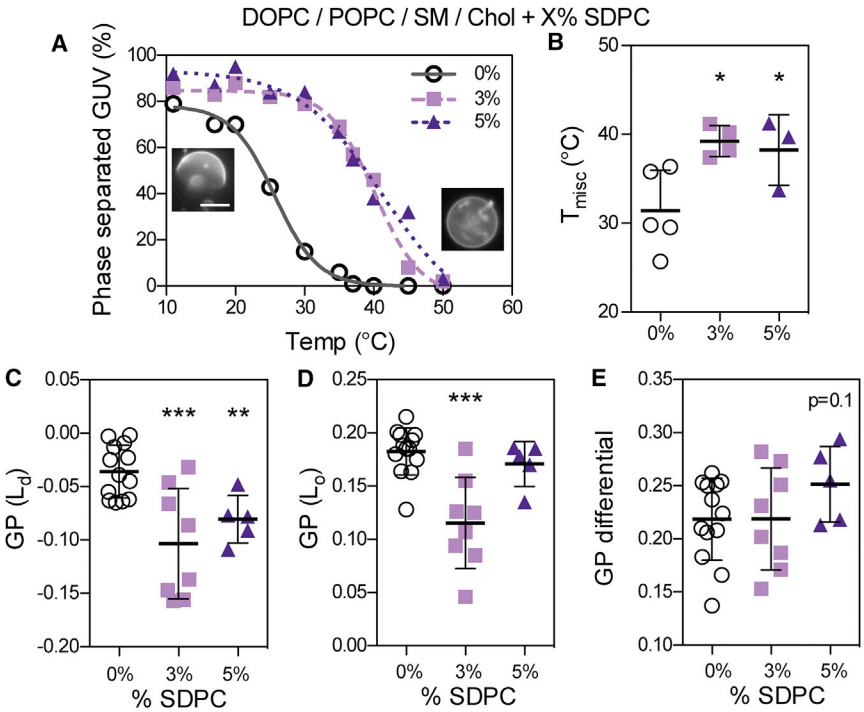

FIGURE 3 Effect of DHA-containing lipids on phase behavior in synthetic GUVs. (*A* and *B*) Inclusion of DHA-containing SDPC resulted in a rightward shift of the phase separation profile of SM/DOPC/POPC/Chol GUVs (*A*), indicative of a significantly increased T_{misc} (*B*). Mean ± SD of three to five experiments; $*p < 0.05$. (*C–E*) As in GPMVs, DHA-bearing lipids decreased the order of L_d domains (*C*), with no notable effect on the L_o phases at higher DHA concentrations (*D*), thereby increasing the GP differential between coexisting domains (*E*). Scale bar, 10 μm. Data in (*C–E*) are mean ± SD from five to 15 vesicles/condition from a single experiment, representative of three independent trials. $*p < 0.05$, $**p < 0.01$, $***p < 0.001$, analyzed by Student's *t*-test compared with 0% SDPC-containing samples. To see this figure in color, go online.

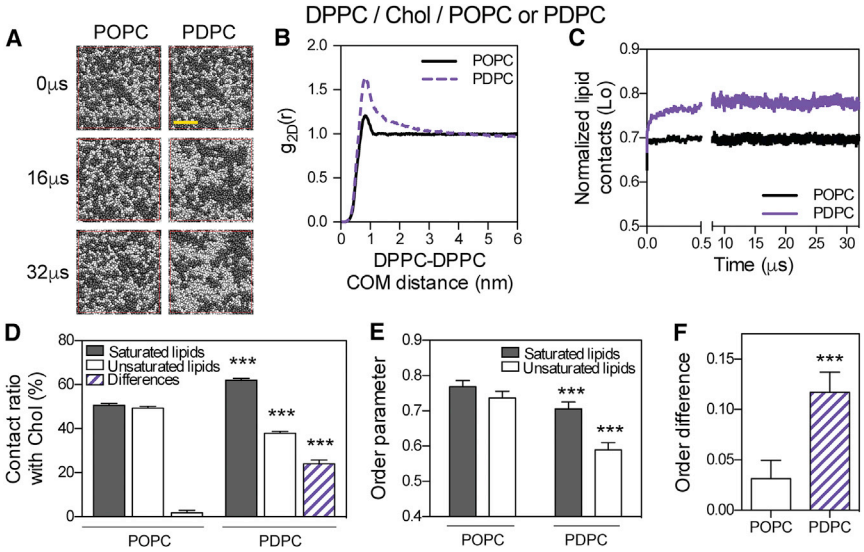

FIGURE 4 DHA-containing lipids stabilize domains by increasing the interdomain difference in MD simulations. (*A*) Snapshots of simulation systems (top view: DPPC and Chol are colored in *black*, and POPC and PDPC are in *white*) at various time points suggest that PDPC-containing membranes form larger domains than POPC. Scale bar (*yellow*), 5 nm. (*B*) 2D radial distribution function of the saturated DPPC center-of-mass (COM) distance confirms more robust segregation of DPPC from disordered lipids in the PDPC membranes. (*C*) Time evolution of total contacts among L_o-forming lipids (DPPC and Chol). L_o contacts increase rapidly and equilibrate at a higher value in PDPC-containing membrane. (*D*) DPPC and POPC interact with Chol equally, whereas in PDPC membranes, DPPC has a much higher frequency of interactions with Chol than PDPC. (*E*) Chain order parameters (based on the second bead of the acyl chain) of saturated (DPPC) and unsaturated (POPC or PDPC) lipids. (*F*) Order differences between ordered (saturated) and disordered (unsaturated) lipids. Data in (*D–F*) are from the last 8 μs of simulation; mean ± SD, analyzed by Student's *t*-test, $***p < 0.001$. To see this figure in color, go online.

interactions extending out beyond 3 nm (>4 molecular diameters; Fig. 4 *B*), the increased number of ordered lipid contacts (Fig. 4 *C*), and the increased preference of Chol for DPPC (Fig. 4 *D*) in the PDPC system. The simulated membranes allowed direct quantification of the lipid acyl chain order parameters that were experimentally investigated by proxy with C-laurdan microscopy in GPMVs (Fig. 2, *D–F*) and GUVs (Fig. 3, *C–E*). In agreement with the inferences from those experiments, the presence of DHA-containing PDPC dramatically decreased the chain order of the unsaturated lipids (Fig. 4 *E*), thereby increasing the interdomain order differential (Fig. 4 *F*). Stabilization of domains by enhanced lipid unsaturation was previously reported based on MD simulations (70) and neutron-scattering experiments (71), and our results are generally consistent with that conclusion.

Exogenous amphiphiles reproduce effects of PUFA lipids

Across model systems ranging from near-atomic simulations to cellular PMs, the inclusion of ω-3 DHA into membrane lipids stabilizes L_o/L_d phase separation by enhancing differences between coexisting domains via disordering of the unsaturated-lipid-rich disordered domains. To determine whether this phenomenon is specific to PUFA incorporation into membrane lipids, we tested the effects of a variety of membrane perturbations on domain order and phase separation. We previously reported that treatment of GPMVs with bile acids enhanced phase separation (23), and we confirmed that effect here for DCA (Fig. 5 *A*). A similar effect was observed for a nonnatural amphiphile, the nonionic detergent Triton X-100 (TX100), which stabilized phase separation in GPMVs by ~4°C at 0.005% (Fig. 5 *B*). The latter result is line with fluorescence resonance energy transfer experiments in synthetic membranes that also showed stabilization of domains by TX100 (72). Both DCA and TX100 treatments also lowered the GP of the disordered phase in GPMVs (Fig. 5 *C*), and thus significantly increased the interdomain order differential (Fig. 5 *D*).

Chol depletion decreases T_{misc} and order of the raft phase

Finally, we tested the effects of Chol depletion by the widely used extraction agent MBCD (73). Chol depletion of RBL cells before GPMV isolation reduced the Chol content in the isolated PMs (Fig. S6) and markedly decreased their phase separation temperature, and both effects progressively increased with increasing MBCD concentrations. This observation was somewhat surprising because it was previously reported that Chol depletion could increase phase separation (2). As a possible explanation for these disparate results, we note that these experiments were done in different cell types, which likely possessed different lipid profiles. Although it is currently impossible to make any meaningful connections between lipidomic features and the phase behavior of complex membranes, synthetic systems do suggest that the effect of Chol concentration on phase separation is nonmonotonic (27), and therefore modulation of Chol concentrations may produce opposing effects in different systems. Moreover, Chol depletion is known to be broadly pleiotropic, affecting a variety of cellular processes, including cytoskeletal organization and

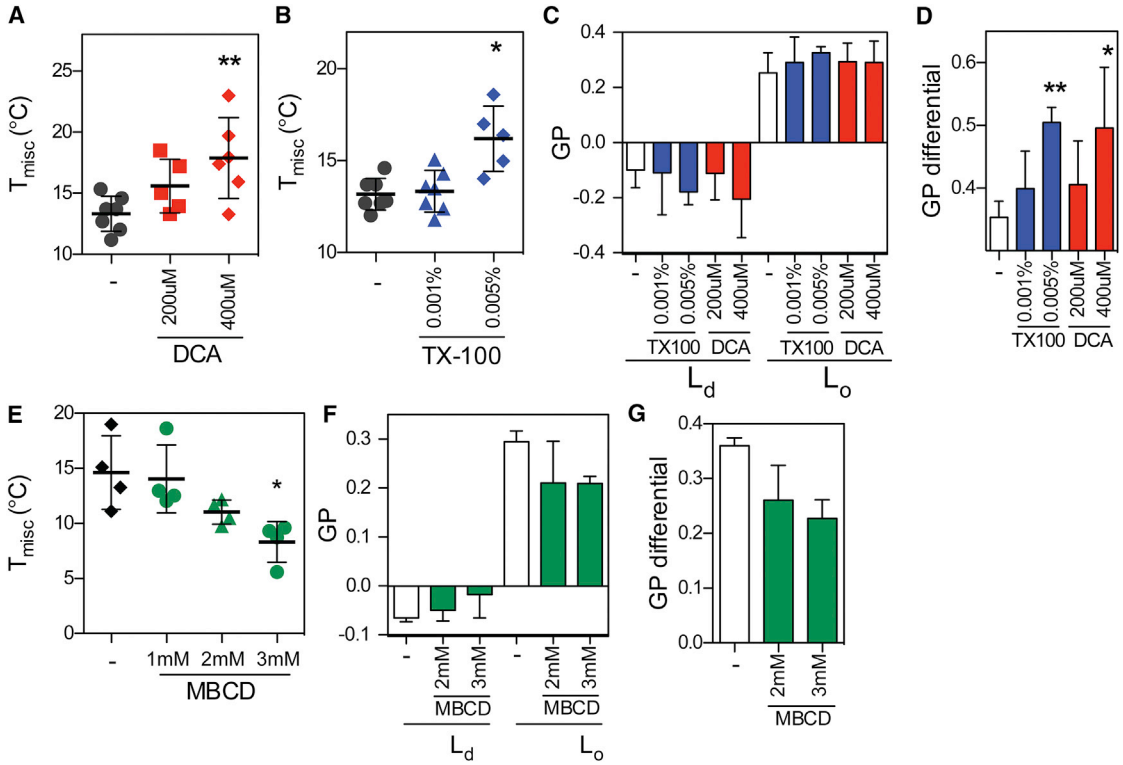

FIGURE 5 Effects of exogenous amphiphiles and Chol depletion on interdomain order differences. (*A* and *B*) Treatment of RBL cells with (*A*) DCA or (*B*) Triton X-100 before GPMV isolation increased T_{misc} in GPMVs. (*C* and *D*) Both TX100 and DCA reduced the GP of the L_d phase (*C*), thereby increasing the order differential between the domains (*D*). (*E*) Acute Chol depletion of RBL cells by MBCD progressively reduced T_{misc}. (*F*) This reduction was associated with an increased L_d phase GP and a decreased L_o phase GP, which combined to lower the interdomain order differential. All data are mean ± SD from three independent experiments and were analyzed by Student's *t*-test. $*p < 0.05$, $**p < 0.01$. To see this figure in color, go online.

signaling (17,73). These effects likely also affect membrane organization in a cell-type-specific manner.

Chol depletion was the only membrane perturbation we attempted that decreased the T_{misc} (Fig. 5 *E*) (this was also the only treatment that had a significant effect on the overall membrane order in GPMVs (Fig. S3)). Consistently, this treatment also had very different effects on the order of the coexisting phases in GPMVs. MBCD weakly increased the order of the L_d phase, but strongly decreased that of the more ordered phase (Fig. 5 *F*), consistent with the expected effect of Chol extraction. In combination, these effects indicate a progressive reduction in the interdomain order differential (Fig. 5 *G*) that correlates with the decreased phase separation temperature (Fig. 5 *E*).

CONCLUSION

Our microscopic measurements of domain order in intact PMs (i.e., GPMVs) across five distinct perturbations allowed us to quantitatively evaluate the relationship between the interdomain order differential and the phase separation temperature. We observed a highly significant correlation ($p < 0.0001$) between these parameters (Fig. 6) regardless of whether the PMs were altered by dietary lipid supplementation (DHA and OA, *orange symbols*), Chol depletion (MBCD, *green symbols*), or exogenous biological (DCA, *red symbols*) or synthetic (TX100, *blue symbols*) amphiphiles. From this relationship and a number of previous

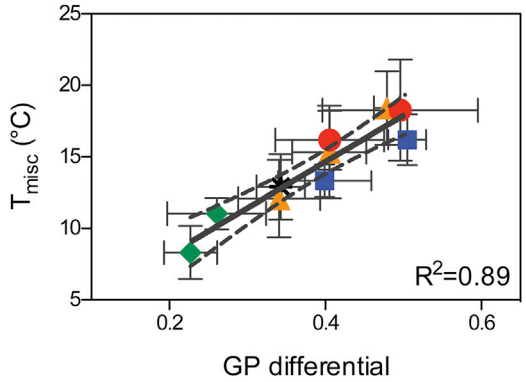

FIGURE 6 The interdomain order differential strongly correlates with phase separation. The effects of all treatments on the interdomain order difference (GP differential) show a strong linear correlation with their effects on T_{misc}, suggesting that the physical differences between coexisting L_o and L_d domains ultimately govern their capacity for phase separation. Black asterisk, untreated; orange triangles, FA-treated; green diamonds, MBCD-treated; blue squares, TX100-treated; red circles, DCA-treated. Data are mean ± SD for all treatments; dashed lines are 95% confidence intervals for the correlation; correlation is significant at $p < 0.0001$. To see this figure in color, go online.

observations (18,26,34,39,64,65,70,71), we conclude that the interdomain order differential is a critical determinant of the phase behavior of biological membranes. Further investigation will be required to determine whether this relationship also holds for other known modulators of phase separation (e.g., protein-protein interactions, protein content in the membrane, and liquid anesthetics). Potential exceptions to the general relationship described in Fig. 6 may be "line-active" compounds, which would be expected to change phase separation without affecting the properties of the coexisting phases.

SUPPORTING MATERIAL

Seven figures are available at http://www.biophysj.org/biophysj/supplemental/S0006-3495(16)30061-3.

AUTHOR CONTRIBUTIONS

I.L. and K.R.L. designed the studies and wrote the manuscript. K.R.L., J.H.L., A.S., M.S., and E.S. performed the experimental work. X.L. and A.A.G. designed and interpreted the computational work.

ACKNOWLEDGMENTS

We thank the Texas Advanced Computing Center for providing computational resources.

This work was supported by the Cancer Prevention and Research Institute of Texas (grant R1215) and the National Institute of General Medical Sciences, National Institutes of Health (grant 1R01GM114282). A.A.G. and X.L. were supported in part by grant R01GM100078 from the National Institute of General Medical Sciences, National Institutes of Health. M.A.S. has paid employment at Lipotype, GmbH.

REFERENCES

1. Lingwood, D., and K. Simons. 2010. Lipid rafts as a membrane-organizing principle. *Science.* 327:46–50.
2. Levental, I., F. J. Byfield, …, P. A. Janmey. 2009. Cholesterol-dependent phase separation in cell-derived giant plasma-membrane vesicles. *Biochem. J.* 424:163–167.
3. Meder, D., M. J. Moreno, …, K. Simons. 2006. Phase coexistence and connectivity in the apical membrane of polarized epithelial cells. *Proc. Natl. Acad. Sci. USA.* 103:329–334.
4. Owen, D. M., D. J. Williamson, …, K. Gaus. 2012. Sub-resolution lipid domains exist in the plasma membrane and regulate protein diffusion and distribution. *Nat. Commun.* 3:1256.
5. Simons, K., and D. Toomre. 2000. Lipid rafts and signal transduction. *Nat. Rev. Mol. Cell Biol.* 1:31–39.
6. Diaz-Rohrer, B. B., K. R. Levental, …, I. Levental. 2014. Membrane raft association is a determinant of plasma membrane localization. *Proc. Natl. Acad. Sci. USA.* 111:8500–8505.
7. Levental, I., D. Lingwood, …, K. Simons. 2010. Palmitoylation regulates raft affinity for the majority of integral raft proteins. *Proc. Natl. Acad. Sci. USA.* 107:22050–22054.
8. Levental, I., M. Grzybek, and K. Simons. 2010. Greasing their way: lipid modifications determine protein association with membrane rafts. *Biochemistry.* 49:6305–6316.
9. Barua, D., and B. Goldstein. 2012. A mechanistic model of early FcεRI signaling: lipid rafts and the question of protection from dephosphorylation. *PLoS One.* 7:e51669.
10. Nicolau, D. V., Jr., K. Burrage, …, J. F. Hancock. 2006. Identifying optimal lipid raft characteristics required to promote nanoscale protein-protein interactions on the plasma membrane. *Mol. Cell. Biol.* 26:313–323.
11. Suzuki, K. G. 2012. Lipid rafts generate digital-like signal transduction in cell plasma membranes. *Biotechnol. J.* 7:753–761.
12. Stone, M. B., and S. L. Veatch. 2015. Steady-state cross-correlations for live two-colour super-resolution localization data sets. *Nat. Commun.* 6:7347.
13. Moens, P. D., M. A. Digman, and E. Gratton. 2015. Modes of diffusion of cholera toxin bound to GM1 on live cell membrane by image mean square displacement analysis. *Biophys. J.* 108:1448–1458.
14. Eggeling, C., C. Ringemann, …, S. W. Hell. 2009. Direct observation of the nanoscale dynamics of membrane lipids in a living cell. *Nature.* 457:1159–1162.
15. Baumgart, T., A. T. Hammond, …, W. W. Webb. 2007. Large-scale fluid/fluid phase separation of proteins and lipids in giant plasma membrane vesicles. *Proc. Natl. Acad. Sci. USA.* 104:3165–3170.
16. Sezgin, E., H. J. Kaiser, …, I. Levental. 2012. Elucidating membrane structure and protein behavior using giant plasma membrane vesicles. *Nat. Protoc.* 7:1042–1051.
17. Levental, K. R., and I. Levental. 2015. Giant plasma membrane vesicles: models for understanding membrane organization. *Curr. Top. Membr.* 75:25–57.
18. Kaiser, H. J., D. Lingwood, …, K. Simons. 2009. Order of lipid phases in model and plasma membranes. *Proc. Natl. Acad. Sci. USA.* 106:16645–16650.
19. Levental, K. R., and I. Levental. 2015. Isolation of giant plasma membrane vesicles for evaluation of plasma membrane structure and protein partitioning. *Methods Mol. Biol.* 1232:65–77.
20. Keller, H., M. Lorizate, and P. Schwille. 2009. PI(4,5)P2 degradation promotes the formation of cytoskeleton-free model membrane systems. *ChemPhysChem.* 10:2805–2812.
21. Johnson, S. A., B. M. Stinson, …, T. Baumgart. 2010. Temperature-dependent phase behavior and protein partitioning in giant plasma membrane vesicles. *Biochim. Biophys. Acta.* 1798:1427–1435.
22. Podkalicka, J., A. Biernatowska, …, A. F. Sikorski. 2015. MPP1 as a factor regulating phase separation in giant plasma membrane-derived vesicles. *Biophys. J.* 108:2201–2211.
23. Zhou, Y., K. N. Maxwell, …, I. Levental. 2013. Bile acids modulate signaling by functional perturbation of plasma membrane domains. *J. Biol. Chem.* 288:35660–35670.
24. Gray, E., J. Karslake, …, S. L. Veatch. 2013. Liquid general anesthetics lower critical temperatures in plasma membrane vesicles. *Biophys. J.* 105:2751–2759.
25. Levental, I., M. Grzybek, and K. Simons. 2011. Raft domains of variable properties and compositions in plasma membrane vesicles. *Proc. Natl. Acad. Sci. USA.* 108:11411–11416.
26. Sezgin, E., T. Gutmann, …, P. Schwille. 2015. Adaptive lipid packing and bioactivity in membrane domains. *PloS One.* 10:e0123930.
27. Veatch, S. L., and S. L. Keller. 2003. Separation of liquid phases in giant vesicles of ternary mixtures of phospholipids and cholesterol. *Biophys. J.* 85:3074–3083.
28. Veatch, S. L., and S. L. Keller. 2002. Organization in lipid membranes containing cholesterol. *Phys. Rev. Lett.* 89:268101.
29. García-Sáez, A. J., S. Chiantia, and P. Schwille. 2007. Effect of line tension on the lateral organization of lipid membranes. *J. Biol. Chem.* 282:33537–33544.
30. Calder, P. C. 2006. n-3 polyunsaturated fatty acids, inflammation, and inflammatory diseases. *Am. J. Clin. Nutr.* 83 (6 Suppl):1505S–1519S.
31. Wang, C., W. S. Harris, …, J. Lau. 2006. n-3 Fatty acids from fish or fish-oil supplements, but not alpha-linolenic acid, benefit

cardiovascular disease outcomes in primary- and secondary-prevention studies: a systematic review. *Am. J. Clin. Nutr.* 84:5–17.

32. Cao, J., K. A. Schwichtenberg, …, M. Y. Tsai. 2006. Incorporation and clearance of omega-3 fatty acids in erythrocyte membranes and plasma phospholipids. *Clin. Chem.* 52:2265–2272.
33. Pinot, M., S. Vanni, …, H. Barelli. 2014. Lipid cell biology. Polyunsaturated phospholipids facilitate membrane deformation and fission by endocytic proteins. *Science.* 345:693–697.
34. Shaikh, S. R., A. C. Dumaual, …, S. R. Wassall. 2004. Oleic and docosahexaenoic acid differentially phase separate from lipid raft molecules: a comparative NMR, DSC, AFM, and detergent extraction study. *Biophys. J.* 87:1752–1766.
35. Soni, S. P., D. S. LoCascio, …, S. R. Wassall. 2008. Docosahexaenoic acid enhances segregation of lipids between : 2H-NMR study. *Biophys. J.* 95:203–214.
36. Wassall, S. R., and W. Stillwell. 2009. Polyunsaturated fatty acid-cholesterol interactions: domain formation in membranes. *Biochim. Biophys. Acta.* 1788:24–32.
37. Pitman, M. C., F. Suits, …, S. E. Feller. 2004. Molecular-level organization of saturated and polyunsaturated fatty acids in a phosphatidylcholine bilayer containing cholesterol. *Biochemistry.* 43:15318–15328.
38. Shaikh, S. R., J. J. Kinnun, …, S. R. Wassall. 2015. How polyunsaturated fatty acids modify molecular organization in membranes: insight from NMR studies of model systems. *Biochim. Biophys. Acta.* 1848 (1 Pt B):211–219.
39. Wassall, S. R., and W. Stillwell. 2008. Docosahexaenoic acid domains: the ultimate non-raft membrane domain. *Chem. Phys. Lipids.* 153:57–63.
40. Georgieva, R., C. Chachaty, …, G. Staneva. 2015. Docosahexaenoic acid promotes micron scale liquid-ordered domains. A comparison study of docosahexaenoic versus oleic acid containing phosphatidylcholine in raft-like mixtures. *Biochim. Biophys. Acta.* 1848:1424–1435.
41. Williams, J. A., S. E. Batten, …, S. R. Wassall. 2012. Docosahexaenoic and eicosapentaenoic acids segregate differently between raft and non-raft domains. *Biophys. J.* 103:228–237.
42. Rockett, B. D., H. Teague, …, S. R. Shaikh. 2012. Fish oil increases raft size and membrane order of B cells accompanied by differential effects on function. *J. Lipid Res.* 53:674–685.
43. Yaqoob, P., E. J. Sherrington, …, P. C. Calder. 1995. Comparison of the effects of a range of dietary lipids upon serum and tissue lipid composition in the rat. *Int. J. Biochem. Cell Biol.* 27:297–310.
44. Pirro, M., P. Mauriège, …, B. Lamarche. 2002. Plasma free fatty acid levels and the risk of ischemic heart disease in men: prospective results from the Québec Cardiovascular Study. *Atherosclerosis.* 160:377–384.
45. Metcalf, R. G., M. J. James, …, L. G. Cleland. 2007. Effects of fish-oil supplementation on myocardial fatty acids in humans. *Am. J. Clin. Nutr.* 85:1222–1228.
46. Ayuyan, A. G., and F. S. Cohen. 2006. Lipid peroxides promote large rafts: effects of excitation of probes in fluorescence microscopy and electrochemical reactions during vesicle formation. *Biophys. J.* 91:2172–2183.
47. Sampaio, J. L., M. J. Gerl, …, A. Shevchenko. 2011. Membrane lipidome of an epithelial cell line. *Proc. Natl. Acad. Sci. USA.* 108:1903–1907.
48. Ejsing, C. S., J. L. Sampaio, …, A. Shevchenko. 2009. Global analysis of the yeast lipidome by quantitative shotgun mass spectrometry. *Proc. Natl. Acad. Sci. USA.* 106:2136–2141.
49. Dimitrov, D. S., and M. I. Angelova. 1988. Lipid swelling and liposome formation mediated by electric fields. *Bioelectrochem. Bioenerg.* 19:323–336.
50. Sezgin, E., D. Waithe, …, C. Eggeling. 2015. Spectral imaging to measure heterogeneity in membrane lipid packing. *ChemPhysChem.* 16:1387–1394.
51. Marrink, S. J., H. J. Risselada, …, A. H. de Vries. 2007. The MARTINI force field: coarse grained model for biomolecular simulations. *J. Phys. Chem. B.* 111:7812–7824.
52. Bulacu, M., N. Goga, …, S. J. Marrink. 2013. Improved angle potentials for coarse-grained molecular dynamics simulations. *J. Chem. Theory Comput.* 9:3282–3292.
53. Bussi, G., D. Donadio, and M. Parrinello. 2007. Canonical sampling through velocity rescaling. *J. Chem. Phys.* 126:014101.
54. Parrinello, M., and A. Rahman. 1981. Polymorphic transitions in single crystals: a new molecular dynamics method. *J. Appl. Phys.* 52:7182–7190.
55. Hess, B., C. Kutzner, …, E. Lindahl. 2008. GROMACS 4: algorithms for highly efficient, load-balanced, and scalable molecular simulation. *J. Chem. Theory Comput.* 4:435–447.
56. Humphrey, W., A. Dalke, and K. Schulten. 1996. VMD: visual molecular dynamics. *J. Mol. Graph.* 14:33–38, 27–28.
57. Yates, C. M., P. C. Calder, and G. Ed Rainger. 2014. Pharmacology and therapeutics of omega-3 polyunsaturated fatty acids in chronic inflammatory disease. *Pharmacol. Ther.* 141:272–282.
58. Teague, H., M. Harris, …, S. R. Shaikh. 2014. Eicosapentaenoic and docosahexaenoic acid ethyl esters differentially enhance B-cell activity in murine obesity. *J. Lipid Res.* 55:1420–1433.
59. Kim, W., Y. Y. Fan, …, R. S. Chapkin. 2008. n-3 polyunsaturated fatty acids suppress the localization and activation of signaling proteins at the immunological synapse in murine CD4+ T cells by affecting lipid raft formation. *J. Immunol.* 181:6236–6243.
60. Sezgin, E., T. Sadowski, and K. Simons. 2014. Measuring lipid packing of model and cellular membranes with environment sensitive probes. *Langmuir.* 30:8160–8166.
61. Kim, H. M., H. J. Choo, …, B. R. Cho. 2007. A two-photon fluorescent probe for lipid raft imaging: C-laurdan. *ChemBioChem.* 8:553–559.
62. Parasassi, T., G. De Stasio, …, E. Gratton. 1991. Quantitation of lipid phases in phospholipid vesicles by the generalized polarization of Laurdan fluorescence. *Biophys. J.* 60:179–189.
63. Owen, D. M., C. Rentero, …, K. Gaus. 2012. Quantitative imaging of membrane lipid order in cells and organisms. *Nat. Protoc.* 7:24–35.
64. Wang, C., M. R. Krause, and S. L. Regen. 2015. Push and pull forces in lipid raft formation: the push can be as important as the pull. *J. Am. Chem. Soc.* 137:664–666.
65. Krause, M. R., T. A. Daly, …, S. L. Regen. 2014. Push-pull mechanism for lipid raft formation. *Langmuir.* 30:3285–3289.
66. Goh, S. L., J. J. Amazon, and G. W. Feigenson. 2013. Toward a better raft model: modulated phases in the four-component bilayer, DSPC/DOPC/POPC/CHOL. *Biophys. J.* 104:853–862.
67. Schäfer, L. V., D. H. de Jong, …, S. J. Marrink. 2011. Lipid packing drives the segregation of transmembrane helices into disordered lipid domains in model membranes. *Proc. Natl. Acad. Sci. USA.* 108:1343–1348.
68. Ingólfsson, H. I., M. N. Melo, …, S. J. Marrink. 2014. Lipid organization of the plasma membrane. *J. Am. Chem. Soc.* 136:14554–14559.
69. Risselada, H. J., and S. J. Marrink. 2008. The molecular face of lipid rafts in model membranes. *Proc. Natl. Acad. Sci. USA.* 105:17367–17372.
70. Ackerman, D. G., and G. W. Feigenson. 2015. Multiscale modeling of four-component lipid mixtures: domain composition, size, alignment, and properties of the phase interface. *J. Phys. Chem. B.* 119:4240–4250.
71. Heberle, F. A., R. S. Petruzielo, …, J. Katsaras. 2013. Bilayer thickness mismatch controls domain size in model membranes. *J. Am. Chem. Soc.* 135:6853–6859.
72. Pathak, P., and E. London. 2011. Measurement of lipid nanodomain (raft) formation and size in sphingomyelin/POPC/cholesterol vesicles shows TX-100 and transmembrane helices increase domain size by coalescing preexisting nanodomains but do not induce domain formation. *Biophys. J.* 101:2417–2425.
73. Zidovetzki, R., and I. Levitan. 2007. Use of cyclodextrins to manipulate plasma membrane cholesterol content: evidence, misconceptions and control strategies. *Biochim. Biophys. Acta.* 1768:1311–1324.